Optimization of P3 Laser Scribing Process in Thin-Film Solar Cells

FIZINIŲ IR TECHNOLOGIJOS MOKSLŲ CENTRAS

Edgaras Markauskas, Paulius Gečys, Gediminas Račiukaitis

edgaras.markauskas@ftmc.lt

Center for Physical Sciences and Technology, Savanoriu Ave. 231, LT-02300, Vilnius, Lithuania

LPM2017

June 5-8, 2017, Toyama, Japan

1. INTRODUCTION

The strongest candidates of the thin-film solar cell technology demonstrate high power conversion efficiency and even can compete with silicon-based solar cells in case of small-scale devices [1]. However, full-scale modules still falls behind the record efficiencies of the mini-cells limiting their commercial success [2].

During the module production the P3 laser scribing step can generate extended heat affected zones adjacent to the laser scribe [3]. In such areas, the laser-induced damage can occur leading to the absorber composition changes and the formation of the electro-conductive secondary phases. Therefore, a non-optimal laser scribing regime would shirt-circuit the cells leading to severe power losses.

The aim of the research was to optimize the P3 laser scribing step in CIGS and CZTSe solar cells. Optimized regime would minimize the induced laser damage and preserve high parallel resistance of individual cells. A wide range of parameters was investigated: laser radiation wavelength was varied from 355 nm to 2.5 µm. Furthermore, femto-, pico-, and nanosecond pulses were investigated. Finally, three different P3 scribing approaches were compared.

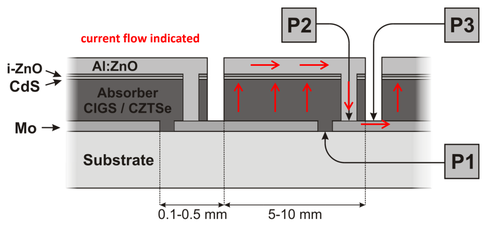

Fig. 1. Regions labeled with P1, P2 and P3 indicate the structuring patterns for the monolithic serial interconnection in CIGS and CZTSe modules.

2. EXPERIMENTAL SETUP

Table 1. Laser systems used in P3 scribing experiments.

Laser	Pulse duration	Wavelength	Rep. rate
Pharos	0.3, 1, 10 ps	1030 nm	500 kHz
Atlantic	13 ps	355, 532, 1064 nm	1 MHz
Atlantic 1342	13 ps	1342 nm	300 kHz
NT277	10 ns	2500 nm	1 kHz

Beam control	ScanLab Scanners	Aerotech XYZ stages
Optics	80 mm f-theta	50 mm

Samples

- Complete structure solar cells:
  1) **CIGS:** (**ZnO:Al/i-ZnO/CdS/CIGS/Mo/Po**).
  2) **CZTSe:** (**ZnO:Al/i-ZnO/CdS/CZTSe/Mo/Glass).**

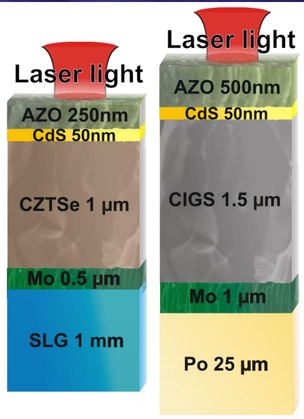

Fig. 2. Schematic cross-sections of CIGS and CZTSe solar cell samples used in experiments.

3. THREE P3 SCRIBE APPROACHES INVESTIGATED

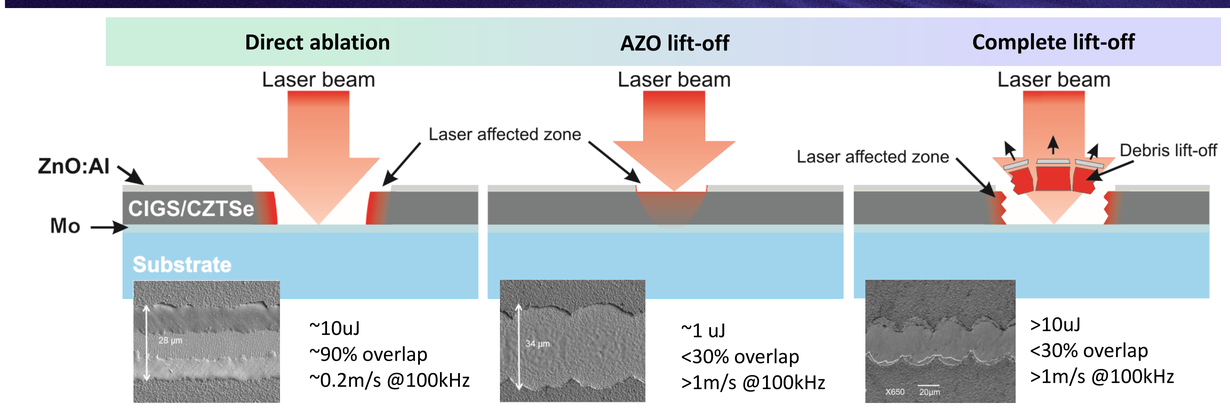

Fig. 3. Direct ablation, AZO lift-off, and complete lift-off P3 approaches investigated in CIGS and CZTSe solar cell samples.

4. LINEAR LASER SCRIBING TECHNIQUE (LLST)

LLST technique provides information about the parallel conductivity of laser P3 scribes [1]. Technique includes performing linear laser scribes and the measurements of cell's parallel conductance. Scribe conductivity can be extracted from the scribe length l and cell conductance G_p^{SC} relationship: $G_p^{SC} = \sigma_{SCM} \cdot l$, where σ_{SCM} is the conductivity of the P3 scribe.

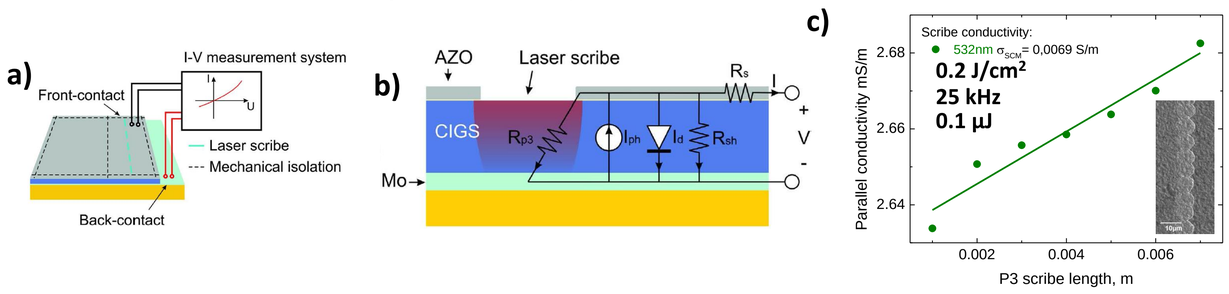

Fig. 4. (**a**) The setup of the linear laser scribing technique (LLST). (b) Typical equivalent circuit model of the laser scribed thin-film solar cell. (c) Result of the LLST measurement.

5. SERIAL INTERCONNECT SIMULATION

Solar cell mini-module simulations were conducted to predict behavior of the laser scribed module efficiency. PV cell array consisting of n cells interconnected via n-1 isolation P3 scribes was simulated. Simulations were based on the parameters of CIGS and CZTSe solar cells presented in Table 2.

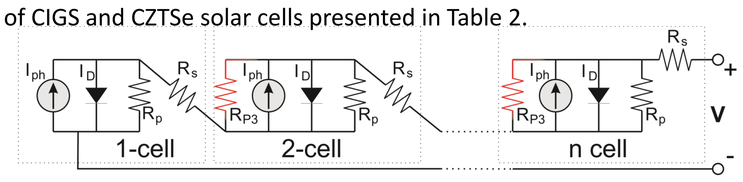

Fig. 5. Equivalent circuit of a n-cell mini-module interconnected in series.

Diode equation for illuminated solar cell:

$$I = I_{ph} - I_0\left(e^{q(V+IR_s)/nkT} - 1\right) - \frac{V + IR_s}{R_p},$$

$$R_{p\,3} = \frac{\rho}{L}, \qquad \frac{1}{R_p} = \frac{1}{R_{sh}} + \frac{L}{\rho},$$

ρ – resistivity of P3 scribe

Sample	eff, %	Voc, mV	Jsc, mA/cm²	Rs, Ohm*cm²	Rp, Ohm*cm²	J0, A/cm²
CIGS [4]	21.7	746	36.6	0.32	1750	$2.4 \cdot 10^{-11}$
CZTSe [5]	9.7	408	38.9	1.44	3130	$1.6 \cdot 10^{-5}$

Table 2. CIGS [4] and CZTSe [5] solar cell parameters used in the mini-module simulations.

6. OPTIMIZATION OF LASER PULSE DURATION

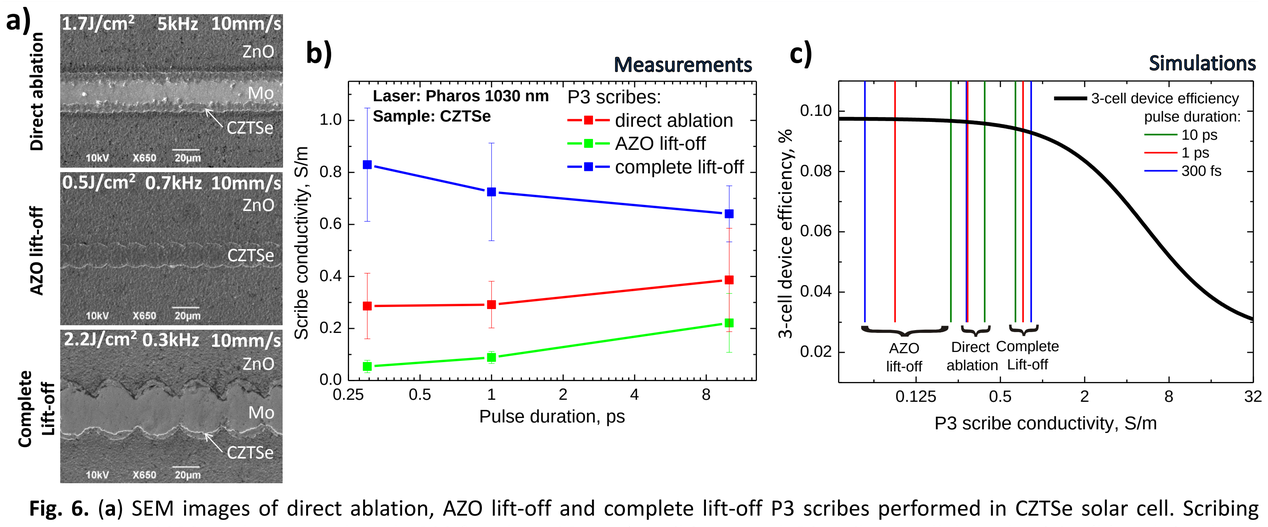

Fig. 6. (**a**) SEM images of direct ablation, AZO lift-off and complete lift-off P3 scribes performed in CZTSe solar cell. Scribing parameters: 1030 nm laser wavelength, 300 fs pulses, 10 mm/s scribing speed. P3 scribe parallel conductivity (**b**) and simulated module efficiency (**c**) dependence on the laser pulse duration.

7. OPTIMIZATION OF LASER RADIATION WAVELENGTH

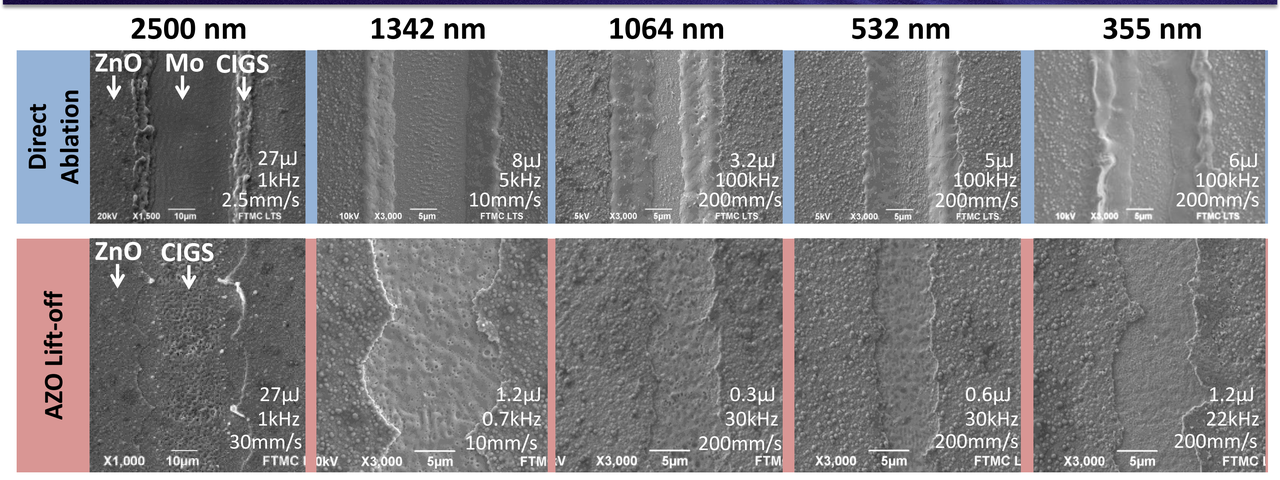

Fig. 7. SEM images of P3 direct ablation and AZO lift-off channels in CIGS structure. Trenches were ablated with 355, 532, 1064, 1342 nm, and 2.5 µm wavelength laser pulses. Two pulse durations investigated: 6 ns (2.5 µm wavelength) and 13 ps (355 - 1342 nm wavelengths).

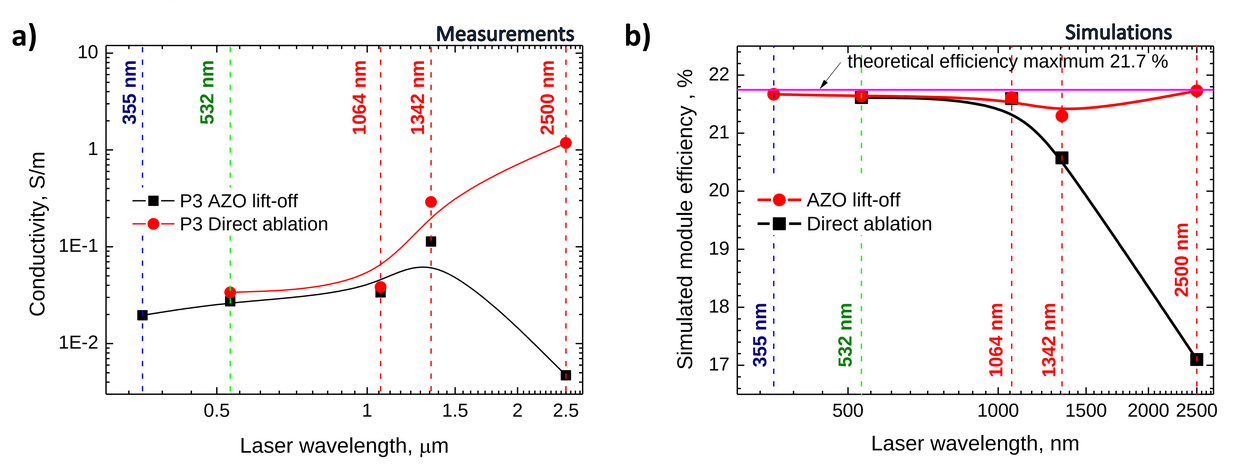

Fig. 8. (**a**) P3 scribe parallel conductivity dependence on the laser wavelength. (**b**) Simulated module efficiency based on extracted P3 conductivity results. Cases of P3 direct ablation and AZO lift-off presented.

8. OPTIMIZATION OF LASER REPETITION RATE

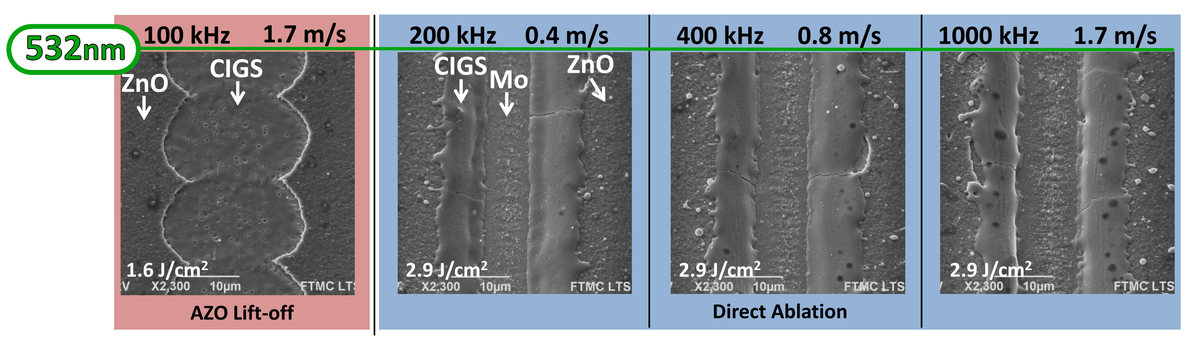

Fig. 9. SEM images of the P3 scribes ablated with 532 nm, 13 ps laser radiation. In the case of direct ablation the P3 scribing speed was varied from 0.4 to 1.7 m/s. Repetition rate was changed from 200 kHz to 1 MHz to maintain constant pulse overlap of 90 %. P3 AZO lift-off scribing parameters: 100 kHz repetition rate, 1.7 m/s scribing speed and 23 % pulse overlap.

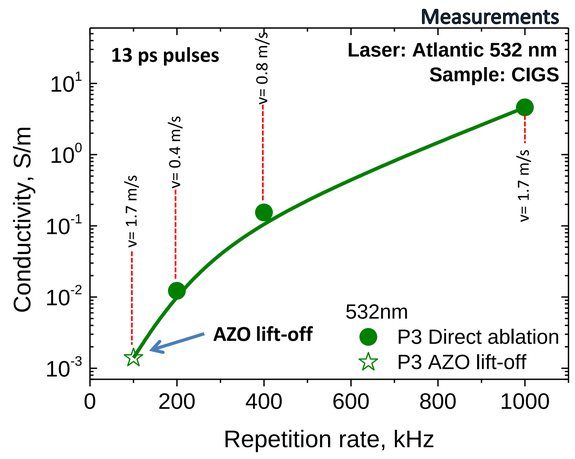

Fig. 10. Laser scribe conductivity dependence on the laser repetition rate. P3 direct ablation and AZO lift-off cases presented. Laser pulse duration 13 ps, laser wavelength 532 nm.

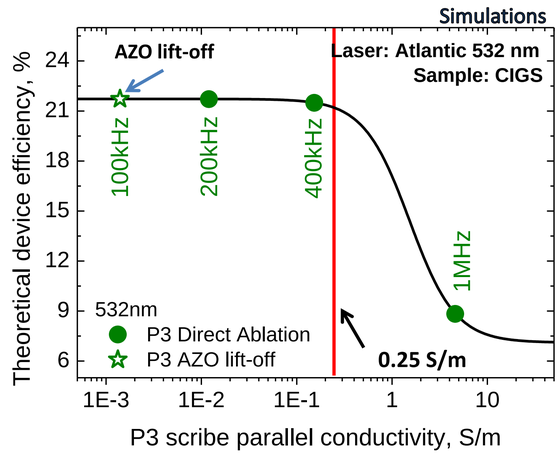

Fig. 11. Simulation of the CIGS 7-cell mini-module efficiency dependence on the conductivity of the P3 sribe.

9. SUMMARY

1. It was shown that the conductivity of direct ablation and AZO lift-off P3 scribes was inversely proportional to the laser pulse duration. The least conductive scribe was achieved using AZO lift-off approach with shortest 300 fs pulses. The complete lift-off was the most conductive scribe showing direct dependence on the used pulse duration in CZTSe cell. High scribe conductivity and high process sensitivity to the absorber material showed the complete lift-off process to be unfavourable for the scribing of P3 channels.
2. In case of AZO lift-off the picosecond laser working at 355 nm and nanosecond laser working at 2.5 µm radiation wavelengths showed the best results (least conductive scribes). In case of direct ablation approach, the damage to the cell performance was more significant, especially at the longer wavelengths.
3. Direct ablation technique showed high scribe conductivity dependence on the laser repetition rate. It was associated with significant heat accumulation effects reaching 7.9 S/m scribe conductivity at 1 MHz rep. rate and 1.7 m/s scribing speed. AZO lift-off approach showed the most promising results with the scribe conductivity of 0.003 S/m at the same scribing speed and 100 kHz rep. rate.
4. Results showed that the P3 AZO lift-off approach is the only solution for low laser-induced damage P3 patterning.

10. ACKNOWLEDGEMENTS

The research leading to these results was partially funded by the European Union FP7 Program under grant agreement No 609355.

REFERENCES

[1] E. Markauskas, P. Gečys, A. Žemaitis, M. Gedvilas, G. Račiukaitis, Validation of Monolithic Interconnection Conductivity in Laser Scribed CIGS Thin-Film Solar Cells, Solar Energy, vol. 120, pp. 35-43, (2015).

[2] S. Dongaonkar, M.A. Alam, In-Line Post-Process Scribing for Reducing Cell to Module Efficiency Gap in Monolithic Thin-Film Photovoltaics, IEEE Journal of Photovoltaics, vol. 4, pp. 324-332, (2014).

[3] T. Bucher, G. Brandal, H. Chen, et al., Quantifying the heat affected zone in laser scribing of thin film solar cells, Manufacturing Letters, vol. 13, pp. 11-14, (2017).

[4] P. Jackson, D. Hariskos, R. Wuerz, et al., Properties of Cu(In,Ga)Se2 solar cells with new record efficiencies up to 21.7%, Physica Status Solidi (RRL) – Rapid Research Letters, 9(1): 28-31 (2015).

[5] G. Brammertz, , M. Buffière, S. Oueslati, et al., Characterization of defects in 9.7% efficient $Cu_2ZnSnSe_4$-CdS-ZnO solar cells, Appl. Phys. Lett. 103, 163904 (2013).